

Magnetic Anisotropy in the Molecular Complex V_{15}

N.P. Konstantinidis

Department of Physics and Department of Mathematics, Trinity College, Dublin 2, Ireland

D. Coffey*

Department of Physics, State University of New York at Buffalo, Amherst, NY 14260

(November 7, 2018)

We apply degenerate perturbation theory to investigate the effects of magnetic anisotropy in the magnetic molecule V_{15} . Magnetic anisotropy is introduced via Dzyaloshinskii-Moriya (DM) interaction in the full Hilbert space of the system. Our model provides an explanation for the rounding of transitions in the magnetization as a function of applied field at low temperature, from which an estimate for the DM interaction is found. We find that the calculated energy differences of the lowest energy states are consistent with the available data. Our model also offers a novel explanation for the hysteretic nature of the time-dependent magnetization data.

PACS numbers: 75.10.Jm Quantized Spin Models, 75.50.Ee Antiferromagnetics, 75.50.Xx Molecular Magnets

I. INTRODUCTION

Magnetic molecules have attracted significant attention in recent years as systems where macroscopic quantum phenomena are displayed, such as relaxation by tunneling of magnetization through a potential well [1]- [4]. These molecules form crystals with very weak intermolecular interactions, thus experiments reflect directly the properties of individual molecules, which can be described by magnetic Hamiltonians. The most studied molecules are a cluster of manganese ions known as Mn_{12} [5], and clusters with iron ions, Fe_n [6-8].

Mn_{12} and Fe_8 possess strong easy axis anisotropy and their states can be characterized to a very good approximation by $\langle S^z \rangle$, the expectation value of the total spin along the easy axis, z . Their ground state has a total spin $S = 10$, and to a good approximation they are described by a single-spin model, where only the $S = 10$ multiplet states are considered [9,10]. Restriction to the $S = 10$ multiplet reduces drastically the Hilbert space of the problem. Iron atoms also form ferric wheel clusters with predominantly antiferromagnetic interactions. In these the total spin of the ground state is $S = 0$ [11]- [15]. Spin dynamics of Fe_6 and Fe_8 have recently been calculated by Honecker et al. [16] using exact diagonalization.

Another molecule of the same class is a cluster with 15 Vanadium ions, known as V_{15} [17], each of which has $S = \frac{1}{2}$. This is similar to some of the Fe_n systems in that the principal interactions are antiferromagnetic. This system has also been investigated using effective spin models in which sets of spins are replaced by one effective spin. However, effective three-spin models which contain only isotropic terms [18]- [20] can not explain the broadening of the spin transitions as a function of magnetic field in equilibrium magnetization measurements, as was pointed out by Chiorescu et al. [18]. Miyashita and Nagaosa [21] considered a three-spin model for V_{15} which included a term, $\sum_{ij} \alpha_{ij} S_i^z S_j^x$. This term is responsible for the quantum tunneling of magnetization states and for the smoothing out of transitions between magnetization states in applied magnetic fields. However, a more microscopic model is needed if a quantitative comparison with data is to be made. In particular, the tunnel splittings, which are important for magnetic relaxation, are very sensitive to Hilbert space truncation and the full Hilbert space of the molecule has to be taken into account [22]. Here we solve for the lowest energy states using degenerate perturbation theory [23,24] in the full Hilbert space, which has $2^{15} = 32,768$ states.

Apart from the opportunity to study the magnetic properties of finite systems which these systems provide, Leuenberger and Loss [25] have proposed the use of Mn_{12} as a qubit, a quantum bit, in a quantum computer. In this type of application it is important that prepared spin states do not decohere on the time scale of the operations on the system necessary to read, write and carry out the manipulations necessary for a computation. Consequently it is important to understand the mechanisms for magnetic relaxation in these molecules. These mechanisms can be probed by the application of time dependent magnetic fields [26,27].

The magnetic hysteresis studies for V_{15} show so-called “butterfly” curves which are different from the ones of Mn_{12} and Fe_8 [18,28]. This has been explained in terms of spin-phonon interaction using the Landau-Zener model for transitions between two states [29]. However, the low number of phonons at very low temperatures points to a different mechanism for magnetization relaxation, intrinsic to the molecule. Here we examine the role of magnetic anisotropy described by the Dzyaloshinskii-Moriya (DM) interactions as a relaxation mechanism. This interaction arises from

spin-orbit coupling and was introduced by Dzyaloshinskii phenomenologically by using symmetry considerations [30]. Moriya derived it microscopically by extending the Anderson theory of superexchange to include spin-orbit coupling [31]. The DM term arises in low symmetry crystals. The fact that finite systems have surfaces where symmetry is reduced ensures that the DM term is an important part of any microscopic description of magnetic molecules [32]. There are other anisotropy sources such as dipolar and hyperfine fields which have very small magnitudes, about 1 mT and 40 mT respectively [18]. Magnetic anisotropy has also been modeled in Ising Hamiltonians by S^+ and S^- terms to reproduce the experimental data [9,10]. Single site anisotropy terms do not contribute in V_{15} since $\sigma_i^2 = 1$, $i = x, y, z$ for $S = \frac{1}{2}$. Therefore the DM interaction is the leading order anisotropy term for this system.

The model Hamiltonian, which includes a Heisenberg exchange interaction and a DM anisotropy term, is solved here with degenerate perturbation theory [23,24]. It is found that inclusion of the DM terms quantitatively explains the widening of the spin transition in the equilibrium magnetization curve. The DM terms are determined quantitatively by comparing with experimental data of Chiorescu et al. [18], and the resulting splitting of the low energy groups of states is in agreement with experimental estimates, $\sim 10^{-2}$ K. Furthermore, it is shown with a model calculation that the non-equilibrium magnetization curve is intrinsically hysteretic due to the presence of the DM interaction. This interaction leads to rapid oscillations with frequencies given by its magnitude. The form of the hysteresis curve depends on when during these oscillations the magnetic field is reversed.

The paper is organized as follows. In section II we discuss the magnetic description of the V_{15} molecule and in section III we introduce the model including the DM interaction determined by symmetry. In section IV we present the properties of the model and compare with experimental data. Finally in section V we give our conclusions.

II. V_{15}

The chemical structure of V_{15} is given by the formula $K_6 [V_{15}^{IV} As_6 O_{42} (H_2O)] \cdot 8H_2O$ [17,33,34]. There are fifteen V^{IV} ions with spin $S = \frac{1}{2}$ placed in a quasi-spherical layered structure (figure 1). These spins sit on two hexagons with a triangle sandwiched between them and all interactions are antiferromagnetic in the simplest model [17]. The spins in each hexagon are paired via a strong coupling $J \cong 800$ K [34]. These pairs are connected with a nearest neighbor interaction $J' \cong 150$ K. There is also a diagonal interaction $J'' \cong 300$ K. The triangle spins do not interact directly with each other. They interact with spins from the top and bottom hexagons, and the interactions are $J_1 \cong J'$ and $J_2 \cong J''$. The molecule has trigonal symmetry and the space group is $R_{\bar{3}c}$. The unit cell includes two molecules but intermolecular interactions are negligible.

Since all interactions are antiferromagnetic the total spin of the ground state is $S = \frac{1}{2}$. This is in contrast with Mn_{12} and Fe_8 , where $S = 10$. In the absence of anisotropy the ground state is four-fold degenerate, and it is made up of two doublets. The lowest lying excited states form a quartet which is separated from the ground state doublets by ≈ 3.7 K. The splitting between the lowest energy multiplets from the rest of the spectrum has been found from EPR spectra to be ~ 500 K [35]. Magnetic anisotropy leads to tunnel splittings between the two doublets, which are $\sim 10^{-2}$ K [36], in contrast with the very small values for the other two molecules ($\sim 10^{-7} - 10^{-11}$ K). There is no macroscopic quantum tunneling for V_{15} according to the Kramers theorem [37], since the system has an odd number of $S = \frac{1}{2}$ spins and the total spin is half-integer [38], giving a doubly degenerate ground state.

From equilibrium magnetization measurements, it is clear that the ground state has $S \cong \frac{1}{2}$ up to a critical value of the field, where a transition to $S \cong \frac{3}{2}$ is detected [18]. This is true for temperatures smaller than 0.9 K. The broadening of the spin transitions can not be attributed to temperature alone, and various factors like dipolar or nuclear hyperfine field distributions are too small, about 1 mT and 40 mT respectively [18]. This broadening can be explained by anisotropic DM interactions, which were also found to be important for the description of neutron scattering data and EPR measurements in Mn_{12} [39]. More recently, analysis of neutron scattering data on V_{15} by Chaboussant et al. [40] has shown the need to include DM interactions. Garanin and Chudnovsky [41] have suggested that the width of EPR lines could also be explained by dislocations in the crystal lattice. Here we assume that there are no defects in the crystals so that data reflects the properties of the V_{15} clusters.

III. MODEL

A microscopic treatment of the problem of the origin of magnetic anisotropy is considered using the full Hilbert space with $2^{15} = 32,768$ states. This approach based on degenerate perturbation theory makes it possible to include the effect of spin-orbit coupling through the DM interaction. Initially perturbation theory is applied in the absence of magnetic anisotropy. The unperturbed Hamiltonian, H_0 , takes into account the spin singlet-triplet correlations present due to the strength of the bond between alternating pairs of spins in the hexagons being more than twice as

large as any other coupling. The ground state of H_0 is eight-fold degenerate due to uncoupled spins in the triangle (figure 1). Then the perturbation includes the remaining terms for bonds on which exchange constants are smaller. An effective Hamiltonian, H^{eff} , is generated for the degenerate subspace. Since singlet-triplet correlations of the prevalent J bond are built into H_0 , the series expansions generated by perturbation theory are absolutely convergent. Diagonalizing H^{eff} gives the eight lowest energy states of the system which are separated from the next set of states roughly by the energy splitting between singlet and triplet states in H_0 . The Hamiltonian is of the form

$$H = H_0 + \lambda H_1 \quad (1)$$

where λ is the perturbation parameter with

$$H_0 = J(\vec{S}_1 \cdot \vec{S}_2 + \vec{S}_3 \cdot \vec{S}_4 + \vec{S}_5 \cdot \vec{S}_6 + \vec{S}_{10} \cdot \vec{S}_{11} + \vec{S}_{12} \cdot \vec{S}_{13} + \vec{S}_{14} \cdot \vec{S}_{15}) \quad (2)$$

and

$$\begin{aligned} H_1 = & J'(\vec{S}_2 \cdot \vec{S}_3 + \vec{S}_4 \cdot \vec{S}_5 + \vec{S}_1 \cdot \vec{S}_6 + \vec{S}_{11} \cdot \vec{S}_{12} + \vec{S}_{13} \cdot \vec{S}_{14} + \vec{S}_{10} \cdot \vec{S}_{15}) + \\ & J''(\vec{S}_1 \cdot \vec{S}_3 + \vec{S}_3 \cdot \vec{S}_5 + \vec{S}_1 \cdot \vec{S}_5 + \vec{S}_{10} \cdot \vec{S}_{12} + \vec{S}_{12} \cdot \vec{S}_{14} + \vec{S}_{10} \cdot \vec{S}_{14}) + \\ & J_1(\vec{S}_2 \cdot \vec{S}_7 + \vec{S}_7 \cdot \vec{S}_{11} + \vec{S}_4 \cdot \vec{S}_8 + \vec{S}_8 \cdot \vec{S}_{15} + \vec{S}_6 \cdot \vec{S}_9 + \vec{S}_9 \cdot \vec{S}_{13}) + \\ & J_2(\vec{S}_1 \cdot \vec{S}_7 + \vec{S}_7 \cdot \vec{S}_{10} + \vec{S}_3 \cdot \vec{S}_8 + \vec{S}_8 \cdot \vec{S}_{14} + \vec{S}_5 \cdot \vec{S}_9 + \vec{S}_9 \cdot \vec{S}_{12}) \end{aligned} \quad (3)$$

The ground state of the unperturbed Hamiltonian is composed of a singlet at each of the six hexagon pairs. When $\lambda \neq 0$ the perturbation mixes in states where one or more of the pairs are excited and generate the elements of H^{eff} . Since J is a very strong bond, this lowest multiplet of 8 states will be well-separated in energy from the rest of the spectrum, and the low temperature behavior is well described by the eigenfunctions of H^{eff} .

In equation (1) the exchange constants given in [34] are varied when $\lambda = 1$ so that the gap from the doublets to the quartet agrees with the experimental value of ≈ 3.7 K. The following parameters are kept:

$$J = 1, J_1 = J' = \frac{225}{800}J, J_2 = J'' = \frac{350}{800}J \quad (4)$$

The unit for J is 800 K and the energy gap to the excited state with these values is equal to $\Delta_1 = 3.61$ K. Thus, the low energy diagram of V_{15} is as shown in figure 2. $\Delta_0 \sim 10^{-2}$ K is the tunnel splitting between the two doublets. This splitting is not described by the present Hamiltonian. A test for the success of perturbation theory is the calculation of the expectation values of the square of the total spin \vec{S}^2 and its projection on the z axis, S^z , for the calculated wavefunctions. These expectation values are half-integer for S^z and integer for \vec{S}^2 at $\lambda = 1$ with a precision equal to the one used to generate the perturbation expansions (double precision-15 digits). This confirms the success of perturbation theory.

A. Magnetic Anisotropy

The anisotropic interaction between two spins \vec{S}_i and \vec{S}_j due to spin-orbit coupling is [30,31]:

$$\vec{D}_{i,j} \cdot \vec{S}_i \times \vec{S}_j + \vec{S}_i \cdot \mathbf{\Gamma}_{i,j} \cdot \vec{S}_j \quad (5)$$

The first term is the DM interaction and it is first order in spin-orbit coupling and antisymmetric. We refer to $\vec{D}_{i,j}$ as the DM vector. The second term is second order in spin-orbit coupling and symmetric, with $\mathbf{\Gamma}_{i,j}$ a second-rank tensor. Thus the DM vector provides the lowest order anisotropy term.

As a minimal model, the DM interaction will be considered on the J bonds only, the strongest exchange constants in the system. The DM interaction is:

$$\vec{D}_{i,j} \cdot \vec{S}_i \times \vec{S}_j = D_{i,j}^x (S_i^y S_j^z - S_i^z S_j^y) + D_{i,j}^y (S_i^z S_j^x - S_i^x S_j^z) + D_{i,j}^z (S_i^x S_j^y - S_i^y S_j^x) \quad (6)$$

Symmetry operations of the V_{15} molecule, rotations of $\frac{2\pi}{3}$ and $\frac{4\pi}{3}$ around the axis that passes through the centers of the hexagons (z), have to leave the form of the Hamiltonian invariant. This constraints the $\vec{D}_{i,j}$ to be related to one another. If

$$\vec{D}_{1,2} = D_{1,2}^x \hat{x} + D_{1,2}^y \hat{y} + D_{1,2}^z \hat{z} \quad (7)$$

then these three parameters determine the DM interaction in the other two J bonds of the bottom hexagon as:

$$\begin{aligned}\vec{D}_{3,4} &= \frac{1}{2} (-D_{1,2}^x + \sqrt{3} D_{1,2}^y) \hat{x} - \frac{1}{2} (\sqrt{3} D_{1,2}^x + D_{1,2}^y) \hat{y} + D_{1,2}^z \hat{z} \\ \vec{D}_{5,6} &= -\frac{1}{2} (D_{1,2}^x + \sqrt{3} D_{1,2}^y) \hat{x} + \frac{1}{2} (\sqrt{3} D_{1,2}^x - D_{1,2}^y) \hat{y} + D_{1,2}^z \hat{z}\end{aligned}\quad (8)$$

The sites $1, \dots, 6$ are those in the bottom hexagon. Due to absence of reflection symmetry with respect to the triangle plane the DM terms in the upper hexagon will differ from the ones in the lower one. However, to minimize the number of free parameters in the model, $\vec{D}_{10,11} = \vec{D}_{1,2}$. Then from symmetry $\vec{D}_{12,13} = \vec{D}_{5,6}$ and $\vec{D}_{14,15} = \vec{D}_{3,4}$.

In the same manner symmetry determines the elements of $\Gamma_{i,j}$. Considering the symmetric part of the spin-orbit coupling again only on the strong bonds (J), and if

$$\Gamma_{1,2} = \begin{pmatrix} \Gamma_{1,2}^{xx} & \Gamma_{1,2}^{xy} & \Gamma_{1,2}^{xz} \\ \Gamma_{1,2}^{xy} & \Gamma_{1,2}^{yy} & \Gamma_{1,2}^{yz} \\ \Gamma_{1,2}^{xz} & \Gamma_{1,2}^{yz} & \Gamma_{1,2}^{zz} \end{pmatrix}\quad (9)$$

then symmetry determines $\Gamma_{i,j}$ by:

$$\Gamma_{i,j} = U \Gamma_{1,2} U^T\quad (10)$$

where U is a rotation by ϕ around the z axis:

$$U = \begin{pmatrix} \cos\phi & \sin\phi & 0 \\ -\sin\phi & \cos\phi & 0 \\ 0 & 0 & 1 \end{pmatrix}\quad (11)$$

$\Gamma_{3,4}$ and $\Gamma_{5,6}$ are determined in this manner and, as in the case of the DM terms, to minimize the number of free parameters in the model $\Gamma_{10,11} = \Gamma_{1,2}$. Then from symmetry $\Gamma_{12,13} = \Gamma_{5,6}$ and $\Gamma_{14,15} = \Gamma_{3,4}$.

The DM term added to the H_1 term in equation (1) is of the form:

$$\begin{aligned}H_{DM} &= \vec{D}_{1,2} \cdot \vec{S}_1 \times \vec{S}_2 + \vec{D}_{3,4} \cdot \vec{S}_3 \times \vec{S}_4 + \vec{D}_{5,6} \cdot \vec{S}_5 \times \vec{S}_6 + \\ &\vec{D}_{10,11} \cdot \vec{S}_{10} \times \vec{S}_{11} + \vec{D}_{12,13} \cdot \vec{S}_{12} \times \vec{S}_{13} + \vec{D}_{14,15} \cdot \vec{S}_{14} \times \vec{S}_{15}\end{aligned}\quad (12)$$

This term is considered as part of the perturbation, H_1 , and is scaled with the perturbation strength λ . From now on $D^x \equiv D_{1,2}^x$, $D^y \equiv D_{1,2}^y$ and $D^z \equiv D_{1,2}^z$. This minimum model is investigated for magnetic anisotropy and the parameters, D^x , D^y and D^z , are determined by comparing with experiment.

We have found that the symmetric $\Gamma_{i,j}$ terms, which are second order in spin-orbit coupling, have little effect in the magnetization curves. Once we have determined the parameters of the minimal model discussed above, we will return to this point. In the case where the moments lie on an open linear array it is possible to introduce local axes so that the DM term, $\vec{D}_{ij} \cdot \vec{S}_i \times \vec{S}_j$, is absorbed into an effective symmetric term [42]. However, the connectivity of the bonds between the spins on the V sites ensures that this term can not be transformed away in this manner.

IV. RESULTS

The effect of the DM terms in the energy spectra is investigated by varying the strength of D^x , D^y and D^z . The average energies of the two doublets and the quartet are plotted for different values of the \vec{D} vector in figure 3. The changes in the energy become more pronounced as $|\vec{D}|$ increases. However, one sees that even DM terms ~ 100 K lead to energy shifts ~ 20 K. The deviations from the average energies of the two doublets are plotted in figure 4, while for the quartet in figure 5. It can be seen that even when $|\vec{D}| \sim 100$ K the sizes of the energy splittings in the two doublets and the quartet are modest. This suggests that the energy level differences estimated from the experiment are comparatively insensitive to \vec{D} so that it can not alone determine \vec{D} .

These spectra arise from the form of the effective Hamiltonian for the triangle spins, H^{eff} , calculated with perturbation theory. The effective Hamiltonian for the triangle spins is of the form $H^{eff} = H^{diag} + H^{off-diag}$, where H^{diag} is a constant diagonal matrix in the basis of total S^z states which is three orders of magnitude larger than the terms in $H^{off-diag}$ and depends on the magnitude of the anisotropy term, as can be seen in figure 3. All the total

S^z sectors of the triangle spins are coupled in $H^{off-diag}$ even when the anisotropy term is $\vec{D}^z \cdot \sum_{ij} \vec{S}_i \times \vec{S}_j$ on the 800 K hexagonal bonds, case (I) in figure 4 and figure 5.

By contrast, when one considers a three-spin model with a Heisenberg coupling, $J_0 \sum_{ij} \vec{S}_i \cdot \vec{S}_j$, and an anisotropy term, $\vec{D}^z \cdot \sum_{ij} \vec{S}_i \times \vec{S}_j$, between the triangle spins, the quartet remains degenerate while the doublets are split into time-reversed pairs separated by $\sqrt{3}D^z$. Unlike the result of this three-spin model, the energies of all quartet levels are changed by the anisotropy term, as can be seen from figures 4 and 5, and the splitting of the higher energy multiplet is larger than the low energy one. This points to the difficulty in understanding the effect of the anisotropy terms on H^{eff} in terms of a simple model for the triangle spins. More generally it supports the conclusions of De Raedt et al. [22] on the dangers of Hilbert space truncation.

A. Magnetization

The magnetization of V_{15} was calculated for various magnetic fields and temperatures as a function of the DM terms. In the absence of DM terms and at zero temperature, S^z is a good quantum number and the magnetization stays constant except at critical fields where there are level crossings. In the first level crossing the ground state selects the state of the zero field ground state doublet with the higher expectation value of the spin, while in the second it switches from this doublet to one of the quartet states. When the temperature differs from zero, the jumps are smeared out and at high enough temperatures there are no sudden changes in the magnetization.

When the DM terms are non-zero at zero temperature \vec{S}^2 does not commute with the Hamiltonian, and the same is true for S^z if either D^x or D^y is non-zero. The magnetization along the field was calculated for $D^x = 50$ K and $D^x = 100$ K at a very low temperature, $T = 0.001$ K, in the case of a field along the x axis and a field along the z axis and is plotted in figure 6. The gyromagnetic ratio used is $g = 2.0023$ [43]. It is observed that the magnetization depends on the degree of anisotropy, D^x . In addition, it is seen that the jump is more smeared out as the magnitude of D^x increases from 0 to 100 K. Magnetic anisotropy is demonstrated by the dependence of the magnetization along the direction of the field on the direction of the field itself.

The broadening of the spin transition can also be observed in figure 7. There the magnetization $\langle S^z \rangle$ is plotted as a function of the magnetic field for four different temperatures and a DM term of magnitude $\sqrt{3}$ 100 K. The magnetization curve is almost identical for $T = 0.001$ K and $T = 0.1$ K. This shows that the broadening of the transition is not a temperature effect, but it is associated with the DM terms. For high enough temperatures the susceptibility is almost constant with the field.

In figure 8 the calculated magnetization is plotted for three different values of D^x with $D^y = D^z = 0$. It is seen that the width of the transition gets bigger with the increase of the DM terms. The origin of the width can be seen in the energy spectrum plotted in figure 9. The presence of matrix elements between the states in the vicinity of the transition field (~ 3 T) leads to level anticrossings. Pairs of degenerate states from the lower multiplet in zero field split up with one hybridizing with a member of the quartet multiple with $S^z \approx \frac{3}{2}$, while the other has no matrix element with this state.

The width of the magnetization transition is an indication of the effect of the DM terms, as can be seen from figures 7 and 8. The transition is characterized by its midpoint $B_{transition}$ and width-difference ΔB in magnetic field values where it has changed by 10 % from its low and high field average spin values on either side of the transition. The results for various DM terms are shown in table I, where it can be seen that $B_{transition}$ depends sensitively on the form of the DM terms. This dependence on the DM terms is illustrated in figure 10 where we plot $B_{transition}$ versus ΔB for two different forms of the DM vector, one in which $D^x \neq 0$ K, $D^y = D^z = 0$ and the other in which $D^z \neq 0$ K, $D^x = D^y = 0$. The values of $B_{transition}$ and the corresponding values of ΔB shown are for different magnitudes of D^x and D^z at two different temperatures. Although the magnetization curves for these two temperatures appear to lie on top of one another in figure 7, there is a difference which should be taken into account in quantitative comparison with data. The effect of increasing temperature is seen to push $B_{transition}$ to higher fields, while ΔB is seen to be non-monotonic. For small magnitudes of the DM term ΔB is larger at $T = 0.1$ K than at $T = 10^{-3}$ K but this is reversed for a sufficiently large magnitude depending on the two forms considered.

These temperature dependences can be understood as follows. $B_{transition}$ moves to higher applied fields with increasing temperature because the higher energy low magnetization state contributes significantly to the thermodynamic average for larger energy differences between the ground and excited state, that is for larger applied fields beyond the field at which the two states are degenerate. The temperature dependence of ΔB is more complicated. Both the temperature and the \vec{D}_{ij} vectors contribute to ΔB . Because the temperatures considered here are so low compared to the variation in the magnitudes of the \vec{D}_{ij} vectors, the difference in the smearing effects of the different temperatures, $\simeq 0.1$ K, can be neglected compared to that due to the hybridization of the levels near $B_{transition}$. The

increase in ΔB for $T = 10^{-3}$ K compared to $T = 0.1$ K arises because the transition takes place at lower values of the applied field at $T = 10^{-3}$ K, ~ 2.60 T, instead of ~ 2.68 T at $T = 0.1$ K, and because the effect of the \vec{D}_{ij} vectors is larger at lower values of the applied field once the energy levels are close. The matrix elements associated with the \vec{D}_{ij} vectors are larger compared to the Zeeman energies in the effective Hamiltonian. As a result increasing the magnitude of \vec{D}_{ij} vectors leads to a larger effect on ΔB at lower temperatures. It was also observed that the results do not depend on the sign of the DM terms.

The above results were calculated with a gyromagnetic ratio $g = 2.0023$. A similar analysis for experimentally determined temperature dependence of the magnetization at $T = 0.1$ K gives $\Delta B = 0.77 \pm 0.10$ T and $B_{transition} = 2.84 \pm 0.05$ T [18]. In order to compare with this data, an average of the values found from EPR spectra for the gyromagnetic ratio is used [17]. They are $g_a = g_b = 1.95$ and $g_c = 1.98$, where a , b and c are the crystallographic axes of the molecule. Using $g = 1.97$ and $D^x = 70$ K, $D^y = D^z = 0$, it is found that $\Delta B = 0.75$ T and $B_{transition} = 2.81$ T, which is within the uncertainty of the experimental value. Therefore, the inclusion of DM terms accounts for the rounding of the magnetization at very low temperatures and provides a description of the magnetic anisotropy of V_{15} . In addition, the gap between the doublets and quartet, ~ 3.7 K, is consistent with the estimates given by Chiorescu et al. [18] and Chaboussant et al. [40] for the effective coupling of the spins in the triangle, induced by interactions between these and the spins in the hexagons. Both groups found $J_0 \simeq 2.4$ K which gives a gap $\frac{3}{2}J_0 \simeq 3.7$ K. We also found that the tunnel splitting between the two doublets is $\Delta_0 = 13$ mK, in agreement with the $\sim 10^{-2}$ K estimate [36]. This is an order of magnitude smaller than the estimates given by Chiorescu et al. [28] (~ 0.05 K) or Chaboussant et al. (~ 0.1 K). We note that the calculated splittings of the quartets, shown in figure 5, are an order of magnitude larger than those of the doublets, shown in figure 4, which may account for the discrepancy between experimental estimates and our results.

In arriving at the form and magnitude of the \vec{D}_{ij} we have relied on a simple model in which the \vec{D}_{ij} are non-zero only on the strongest bonds and it is not obvious how model dependent our results are in the absence of more detailed data. The original estimates by Moriya [31] relied on a superexchange model where magnetic order is driven by strong short-range correlations due to strongly suppressed hopping between sites. Estimates of the \vec{D}_{ij} 's then come from considering the mixing of orbitals by angular momentum matrix elements. In V_{15} interactions between ions on hexagon sites are mediated by pairs of oxygen atoms. Depending on whether one of these oxygen atoms is linked to an arsenic atom or another vanadium atom, the Heisenberg coupling is either 800 K or 150 K. In these circumstances it is not clear how reliable estimates are based on the simple tight-binding approach. The magnitude of the \vec{D}_{ij} vectors found here is comparable to the Heisenberg couplings. This is larger than the estimate based on Moriya's original approach which gives $|\vec{D}_{ij}| \sim \frac{\Delta g}{g}$, where Δg is the shift in the gyromagnetic ratio from that of a free electron. However, Katsnelson et al. [39] also found strong Dzyaloshinskii-Moriya interactions with values comparable to the isotropic constants in their analysis, which was based on an effective eight spin model of neutron scattering and EPR data on Mn_{12} .

The determination of \vec{D}_{ij} is carried out in the absence of the symmetric anisotropy term, $\Gamma_{i,j}$. We investigated the effect of including $\Gamma_{i,j}$'s with a range of magnitudes for its elements with different \vec{D}_{ij} 's. Since the \vec{D}_{ij} 's are first order in the spin-orbit interaction while the $\Gamma_{i,j}$'s are second order, we have assumed the magnitudes of the symmetric anisotropy terms to be smaller than the antisymmetric ones. For illustration we show in fig. 11 the dependence of $B_{transition}$ and the corresponding values of ΔB for different forms of $\Gamma_{i,j}$ given in table II. In this case $D^x = 70$ K, $D^y = D^z = 0$ with $g = 2.0023$. One sees that the values of $B_{transition}$ and ΔB are not significantly changed from the values given by the DM terms alone. It was observed here that the results depend on the sign of the $\Gamma_{i,j}$ terms.

B. Magnetic Relaxation

Apart from equilibrium magnetization measurements, the magnetization of V_{15} in a varying external field has been measured. The data shows a so-called "butterfly" hysteresis, where the magnetization initially increases with the field, then reaches a plateau, and eventually approaches saturation [18,28]. This has been attributed to non-equilibrium distribution of phonons, and the spin-phonon mechanism for magnetic relaxation is called "hole-burning". Here the role of DM terms in magnetic relaxation is investigated.

In order to calculate the magnetization in a swept field as in the experiments it is necessary to calculate the density matrix for the eight low energy states. However, this is a prohibitively expensive numerical calculation if one is to reach applied fields of 7 T with the sweeping rate of 0.14 T/s. This is because the characteristic time, $\tau_0 = \frac{\hbar}{k_B K} = 7.64 \times 10^{-12}$ s, associated with anisotropy terms is so short compared to the ~ 50 s required to reach 7 T, that the number of time steps needed is very large. The presence of rapidly varying phases in the elements of the density matrix requires a very fine time step $\ll \tau_0$. The computational effort to get accurate results is enormous.

Therefore, rather than consider a time dependent magnetic field which changes at a constant rate, we consider the case in which a 10 T field along the z direction is suddenly switched on, off, or reversed. In the absence of magnetic anisotropy there is no change in $\langle S^z \rangle$ with time. However, this is not the case in the presence of DM terms. As can be seen in figure 9, there is hybridization between the zero field states as a function of applied field, and matrix elements responsible for this lead to a time dependent $\langle S^z \rangle$ when the applied field is suddenly changed.

We illustrate this point by calculating the magnetization for the case where the magnetic field has an initial strength of 10 T, and $D^x = 80$ K, $D^y = 30$ K, $D^z = 0$ and $g = 2.0023$. The ground state magnetization is $\langle S^z \rangle = 1.49$. Then the magnetic field is suddenly switched off, and the evolution of the magnetization is calculated in the basis of the eight lowest states of the same problem in zero magnetic field. Any excited state higher in energy is separated by a gap of order J from the lowest energy manifold, and the probability of the state of the system belonging to this manifold is 0.9997, so this approximation is well justified.

The magnetization varies harmonically with time, as seen in figure 12, and the frequencies of its variation are determined by the energy differences of the system at zero magnetic field. After a time equal to $100\tau_0 \simeq 10^{-10}$ s, the field is turned back on to 10 T and $\langle S^z \rangle$ now varies with different frequencies and amplitude. The presence of more than one frequency in the time dependence points to the inadequacy of a two-level model and suggests that there are significant corrections to any Landau-Zener treatment of the relaxation. The average value of the magnetization is different in the two cases, and in particular the average value after the field is turned on again depends on the wavefunction at the exact moment the field is switched. The origin of this effect is the magnetic anisotropy of the DM terms, a source of magnetic decoherence for the molecule. The calculation can also be done starting from the zero field ground states in a non-zero magnetic field, and after $\sim 10^{-10}$ s switching off the field suddenly. The time dependence is similar to the previous case, and once again the average value of $\langle S^z \rangle$ after the field has been switched off depends on the state of the system at the moment it was switched off. The DM terms therefore provide a source of spin decoherence with a decoherence time $\sim 10^{-12}$ s.

In both cases the calculation was done assuming instantaneously switched on and off fields and demonstrates magnetic decoherence and hysteresis in the presence of DM terms. If a time varying field is introduced in the calculation, the presence of rapidly varying phases requires a very fine time step for the calculation of the time evolution of the magnetization. This time step has to be a fraction of 10^{-12} s, and a calculation of the evolution of the magnetization for realistic times would require an enormous amount of computational effort. However, the small time scale calculation demonstrates the intrinsic magnetic decoherence in the presence of magnetic anisotropy. Hysteresis is seen in experiment and attributed to the spin-phonon interaction [18]. The present mechanism is independent of temperature and can be expected to provide the dominant relaxation process at very low temperatures.

V. CONCLUSION

Degenerate perturbation theory was used to study magnetic anisotropy in the molecule V_{15} . The DM term introduced in the model quantitatively accounts for the rounding of transitions in the magnetization at very low temperatures, their width at midpoint, through the avoided level crossing, as well as observed zero field splitting of the lowest four states.

We have shown that the DM interaction is also responsible for spin decoherence and magnetic hysteresis. This is present even at very low temperatures where thermal mechanisms are absent. This source of decoherence may pose a problem for the application of magnetic molecules in quantum computing, since it is necessary to control the time evolution of states with external magnetic fields and electromagnetic pulses [25]. In order for a molecule with a DM interaction to be suitable for quantum computing it would be necessary to carry out operations on a time scale much shorter than $\frac{\hbar}{\Delta E}$, where ΔE is comparable to the magnitude of the DM interaction. In the present example this is 10^{-12} s.

The use of perturbation theory to calculate the low energy and temperature properties of V_{15} is an alternative to exact diagonalization which has been discussed by Honecker et al. [16] for Fe_6 and Fe_8 . Perturbation theory works particularly well in the case of V_{15} because of the strength of the hexagonal bonds. However, we have also applied perturbation theory to a system of 20 $S = \frac{1}{2}$ spins by calculating the effect of quantum fluctuations around the classical ground state [24]. The dimension of the Hilbert space in that case is almost exactly the same as Fe_8 , $\sim 10^6$. It is possible that this approach will also succeed in systems with larger, more classical moments and larger Hilbert spaces. This would allow a more microscopic approach to the treatment of Mn_{12} , which may resolve some of the questions raised by Zhong et al. [44].

VI. ACKNOWLEDGEMENTS

This work was carried out at the Center for Computational Research at SUNY Buffalo. N.P.K. is supported by a Marie Curie Fellowship of the European Community program Development Host Fellowship under contract number HPMD-CT-2000-00048.

* Current address: Department of Physics, Buffalo State College, 1300 Elmwood Avenue, Buffalo, NY 14222.

-
- [1] A. Caneschi, D. Gatteschi, C. Sangregorio, R. Sessoli, L. Sorace, A. Cornia, M.A. Novak, C. Paulsen and W. Wernsdorfer, *J. Magn. Magn. Mater.* **200**, 182 (1999).
 - [2] J. Villain, in *Frontiers Of Neutron Scattering*, edited by A. Furrer (World Scientific, 2000).
 - [3] W. Wernsdorfer and R. Sessoli, *Science* **284**, 133 (1999).
 - [4] L. Gunther and B. Barbara, Eds., *Quantum Tunneling of Magnetization-QTM '94* (Kluwer, Dordrecht, Netherlands, 1995).
 - [5] A. Caneschi, D. Gatteschi, R. Sessoli, A. Barra, L.C. Brunel and M. Guillot, *J. Am. Chem. Soc.* **113**, 5873 (1991).
 - [6] C. Delfs, D. Gatteschi, L. Pardi, R. Sessoli, K. Wieghardt and D. Hanke, *Inorg. Chem.* **32**, 3099 (1993).
 - [7] C. Sangregorio, T. Ohm, C. Paulsen, R. Sessoli and D. Gatteschi, *Phys. Rev. Lett.* **78**, 4645 (1997).
 - [8] R. Caciuffo, G. Amoretti, A. Murani, R. Sessoli, A. Caneschi and D. Gatteschi, *Phys. Rev. Lett.* **81**, 4744 (1998).
 - [9] M.N. Leuenberger and D. Loss, *Phys. Rev. B* **61**, 1286 (2000).
 - [10] A.L. Barra, P. Debrunner, D. Gatteschi, C.E. Shulz and R. Sessoli, *EuroPhys. Lett.* **35**, 133 (1996).
 - [11] A. Caneschi, A. Cornia, A. C. Fabretti, S. Foner, D. Gatteschi, R. Grandi and L. Schenetti, *Chem. Eur. J.* **2**, 1379 (1996).
 - [12] R.W. Saalfrank, I. Bernt, E. Uller and F. Hampel, *Angew. Chem. Int. Ed. Engl.* **36**, 2482 (1997).
 - [13] D. Gatteschi, A. Caneschi, L. Pardi and R. Sessoli, *Science* **265**, 1054 (1994).
 - [14] K.L. Taft, C.D. Delfs, G.C. Papaefthymiou, S. Foner, D. Gatteschi and S.J. Lippard, *J. Am. Chem. Soc.* **116**, 823 (1994).
 - [15] A. Caneschi, A. Cornia, A.C. Fabretti and D. Gatteschi, *Angew. Chem. Int. Ed. Engl.* **38**, 2774 (1999).
 - [16] A. Honecker, F. Meier, D. Loss and B. Normand, *Eur. Phys. J. B* **27**, 487 (2002).
 - [17] D. Gatteschi, L. Pardi, A.L. Barra, A. Müller and J. Döring, *Nature (London)* **354**, 463 (1991).
 - [18] I. Chiorescu, W. Wernsdorfer, A. Müller, H. Bögge and B. Barbara, *J. Magn. Magn. Mater.* **221**, 103 (2000).
 - [19] I. Rudra, S. Ramasesha and D. Sen, *J. Phys. Condens. Matter* **13**, 11717 (2001).
 - [20] C. Raghun, I. Rudra, D. Sen and S. Ramasesha, *Phys. Rev. B* **64**, 064419 (2001).
 - [21] S. Miyashita and N. Nagaosa, *Prog. Theor. Phys.* **106**, 533 (2001).
 - [22] H.A. De Raedt, A.H. Harns, V.V. Dobrovitski, M. Al-Saqer, M.I. Katsnelson, B.N. Harmon, *J. Magn. Magn. Mat.* **246**, 392 (2002).
 - [23] M.P. Gelfand, *Solid State Commun.* **98**, 11 (1996).
 - [24] N.P. Konstantinidis and D. Coffey, *Phys. Rev. B* **63**, 184436 (2001).
 - [25] M. Leuenberger and D. Loss, *Nature* **410**, 789 (2001).
 - [26] B. Barbara, L. Thomas, F. Lioni, A. Sulpice and A. Caneschi, *J. Magn. Magn. Mater.* **177-181**, 1324 (1998).
 - [27] Y. Zhong, M.P. Sarachik, J. Yoo and D. N. Hendrickson, *Phys. Rev. B* **62**, R9256 (2000).
 - [28] I. Chiorescu, W. Wernsdorfer, A. Müller, H. Bögge and B. Barbara, *Phys. Rev. Lett.* **84**, 3454 (2000).
 - [29] K.W.H. Stevens, *Rep. Prog. Phys.* **30**, 189 (1967).
 - [30] I.E. Dzyaloshinskii, *Zh. Eksp. Teor. Fiz.* **32**, 1547 (1957) [*Sov. Phys. JETP* **5**, 1259 (1957)].
 - [31] T. Moriya, *Phys. Rev.* **120**, 91 (1960).
 - [32] A. Crépieux and C. Lacroix, *J. Magn. Magn. Mater.* **182**, 341 (1998).
 - [33] A. Müller and J. Döring, *Angew. Chem., Int. Ed. Engl.* **27**, 1721 (1991).
 - [34] D. Gatteschi, L. Pardi, A.L. Barra and A. Müller, *Mol. Eng.* **3**, 157 (1993).
 - [35] A.L. Barra, D. Gatteschi, L. Pardi, A. Müller and J. Döring, *J. Am. Chem. Soc.* **114**, 8509 (1992).
 - [36] G.C. Carter, L.H. Bennett and D.J. Kahan, *Prog. Mater. Sci.* **20**, 1 (1977).
 - [37] H.A. Kramers, *Proc. Acad. Sci. Amsterdam* **33**, 959 (1930).
 - [38] W. Wernsdorfer, S. Bhaduri, C. Boskovic, G. Christou and D.N. Hendrickson, *Phys. Rev. B* **65**, 180403 (2002).
 - [39] M.I. Katsnelson, V.V. Dobrovitski and B.N. Harmon, *Phys. Rev. B* **59**, 6919 (1999).
 - [40] G. Chaboussant, R. Basler, A. Sieber, S.T. Ochsenbein, A. Desmedt, R.E. Lechner, M.T.F. Telling, P. Kögerler, A. Müller and H.-U. Güdel, *Europhys. Lett.* **59**, 291 (2002).
 - [41] D.A. Garanin and E.M. Chudnovsky, *Eur. Phys. J. B* **29**, 3 (2002).
 - [42] N.E. Bonesteel, D. Stepanenko and D.P. DiVincenzo, *Phys. Rev. Lett.* **87**, 207901 (2001).
 - [43] M. Kaku, *Quantum Field Theory: A Modern Introduction* (Oxford University Press, 1993).
 - [44] Y. Zhong, M.P. Sarachik, J.R. Friedman, R.A. Robinson, T.M. Kelley, H. Nakotte, A.C. Christianson, F. Trouw, S.M.J. Aubin and D.N. Hendrickson, *J. Appl. Phys.* **85**, 5636 (1999).

TABLE I. Magnetization transition. Index A refers to $T = 0.001$ K, while B to $T = 0.1$ K.

D^x (K)	D^y (K)	D^z (K)	Δ_0 (K)	Δ_1 (K)	ΔB_A (T)	B_{tA} (T)	ΔB_B (T)	B_{tB} (T)
0	0	0	0	3.611	0.08	2.66	0.36	2.69
25	0	0	0.002	3.618	0.30	2.65	0.40	2.70
50	0	0	0.007	3.641	0.65	2.63	0.59	2.69
80	0	0	0.017	3.688	0.96	2.68	0.83	2.77
100	0	0	0.027	3.730	1.19	2.78	1.03	2.86
0	0	100	0	3.618	0.07	2.65	0.36	2.70
20	20	100	0.003	3.648	0.52	2.62	0.52	2.69
30	30	100	0.007	3.685	0.78	2.60	0.71	2.68
40	40	100	0.013	3.736	1.05	2.60	0.89	2.68
50	50	100	0.020	3.801	1.28	2.61	1.11	2.70

 TABLE II. Magnetization transition with inclusion of $\Gamma_{i,j}$ terms. $D^x = 70$ K, $D^y = D^z = 0$ K, $T = 0.001$ K.

point	$\Gamma_{1,2}^{xx}$ (K)	$\Gamma_{1,2}^{yy}$ (K)	$\Gamma_{1,2}^{zz}$ (K)	$\Gamma_{1,2}^{xy}$ (K)	$\Gamma_{1,2}^{xz}$ (K)	$\Gamma_{1,2}^{yz}$ (K)	ΔB (T)	B_t (T)
1*	0	0	0	0	0	0	0.86	2.66
1	0	0	0	0	50	0	0.69	2.69
2	0	0	0	50	50	0	0.71	2.69
3	0	0	0	50	50	50	0.72	2.66
4	0	0	50	20	20	20	0.71	2.60
5	10	10	10	10	10	10	0.77	2.59
6	10	10	10	0	0	20	0.80	2.58
7	0	0	0	20	20	20	0.79	2.66
8	0	0	0	10	10	10	0.81	2.67
9	0	0	0	10	0	0	0.84	2.67
10	0	0	0	50	0	0	0.86	2.67
11	0	0	0	50	0	10	0.86	2.67
12	0	0	0	40	0	20	0.85	2.66
13	0	0	0	0	0	30	0.85	2.65
14	0	0	0	0	0	50	0.86	2.64
15	0	0	0	50	0	50	0.87	2.64

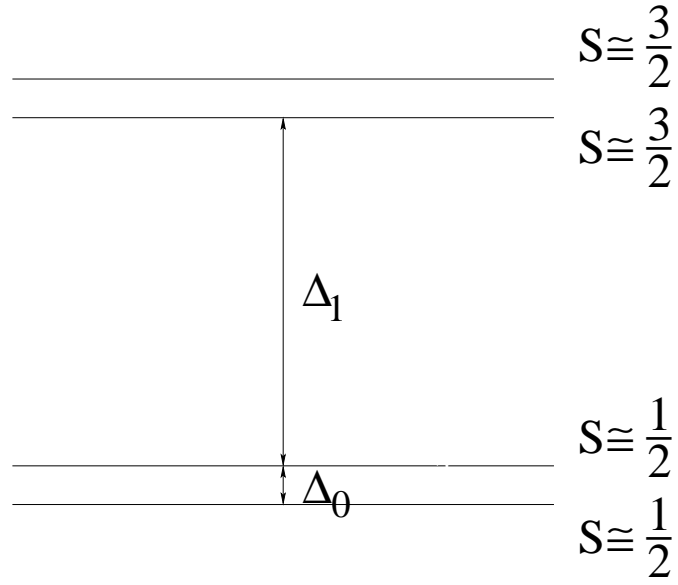


FIG. 2. Low energy diagram for V_{15} .

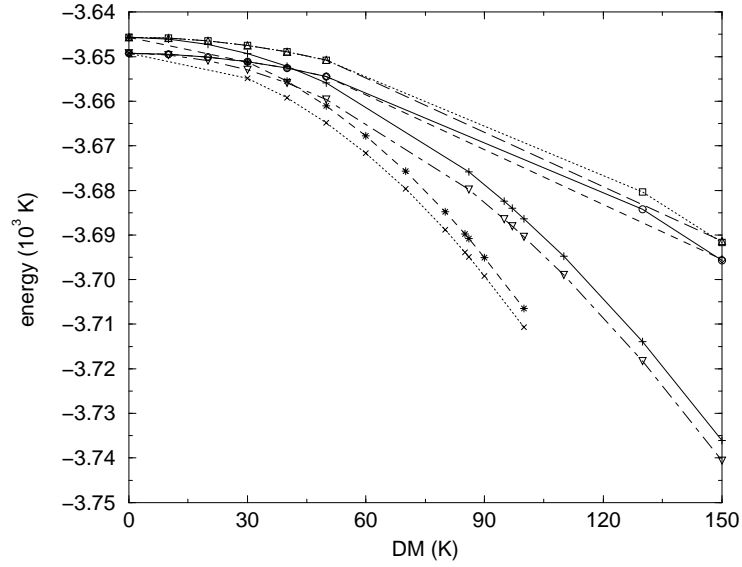


FIG. 3. Average energy for the lowest and the highest multiplet in the D^x, D^y, D^z parameter space:
(I) $D^x=D^y=0, D^z$, \circ : $S = \frac{1}{2}$, \square : $S = \frac{3}{2}$ (II) $D^x, D^y=D^z=0$, \diamond : $S = \frac{1}{2}$, \triangle : $S = \frac{3}{2}$
(III) $D^x=D^y, D^z=0$, ∇ : $S = \frac{1}{2}$, $+$: $S = \frac{3}{2}$ (IV) $D^x=D^y=D^z$ \times : $S = \frac{1}{2}$, $*$: $S = \frac{3}{2}$.

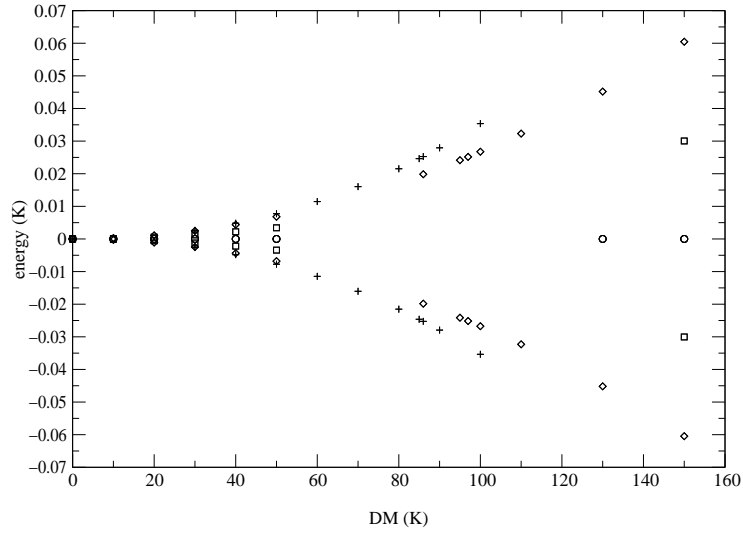


FIG. 4. Deviations from the average energy for the two doublets in the D^x , D^y , D^z parameter space:
(I) \circ : $D^x = D^y = 0$, D^z (K) (II) \square : D^x (K), $D^y = D^z = 0$
(III) \diamond : $D^x = D^y$ (K), $D^z = 0$ (IV) $+$: $D^x = D^y = D^z$ (K).

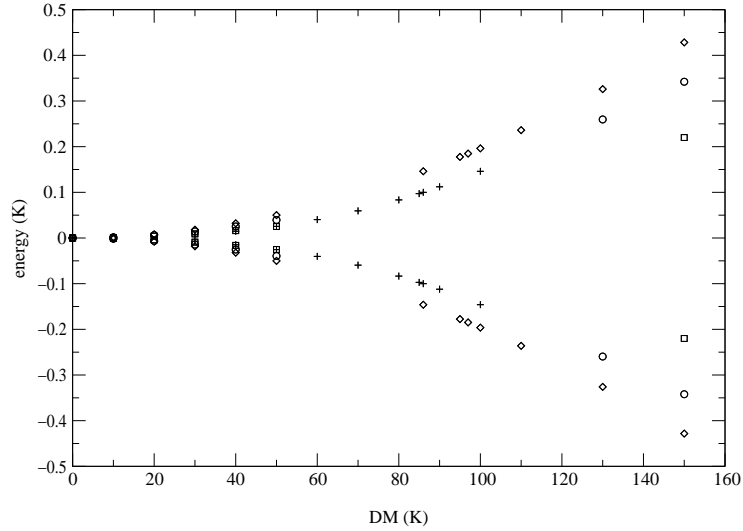


FIG. 5. Deviations from the average energy for the quartet in the D^x , D^y , D^z parameter space:
(I) \circ : $D^x = D^y = 0$, D^z (K) (II) \square : D^x (K), $D^y = D^z = 0$
(III) \diamond : $D^x = D^y$ (K), $D^z = 0$ (IV) $+$: $D^x = D^y = D^z$ (K).

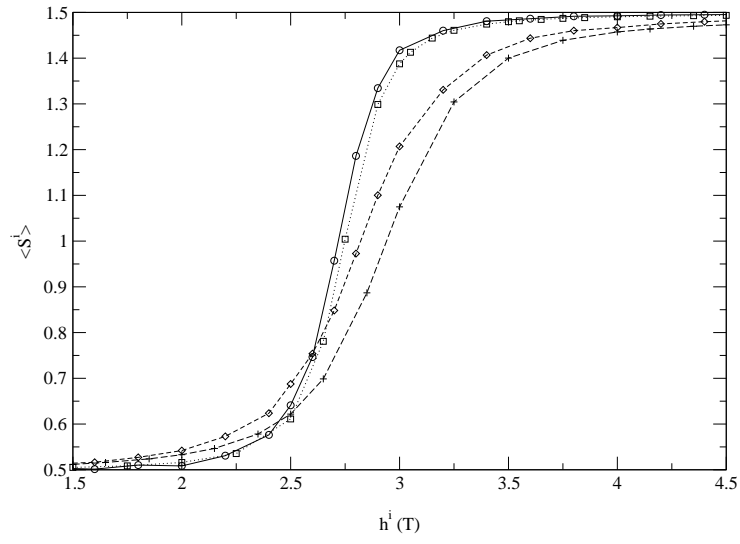


FIG. 6. $\langle S^i \rangle$ vs. h^i , $D^y = D^z = 0$, $T = 0.001$ K: \circ : $i = x$, $D^x = 50$ K, \square : $i = z$, $D^x = 50$ K, \diamond : $i = x$, $D^x = 100$ K, $+$: $i = z$, $D^x = 100$ K.

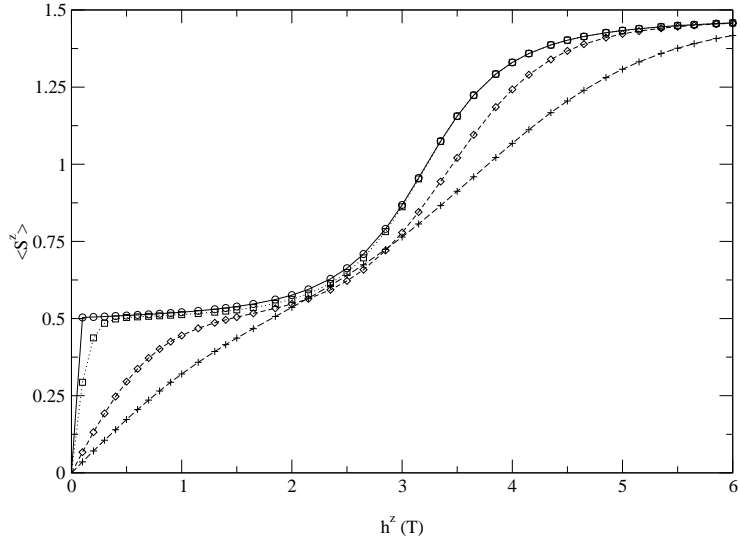


FIG. 7. $\langle S^z \rangle$ vs. h^z , $D^x = D^y = D^z = 100$ K, \circ : $T = 0.001$ K, \square : $T = 0.1$ K, \diamond : $T = 0.5$ K, $+$: $T = 1$ K.

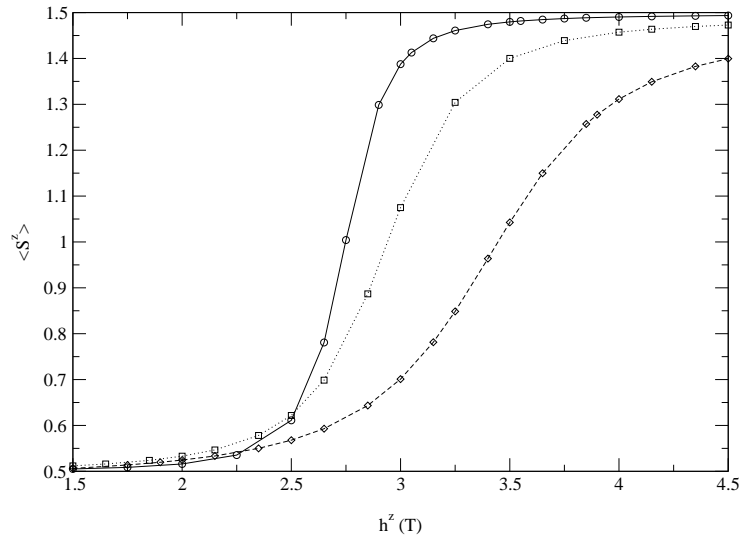


FIG. 8. $\langle S^z \rangle$ vs. h^z , $T = 0.001$ K, $D^y = D^z = 0$ K, \circ : $D^x = 50$ K, \square : $D^x = 100$ K, \diamond : $D^x = \sqrt{3} \cdot 100$ K.

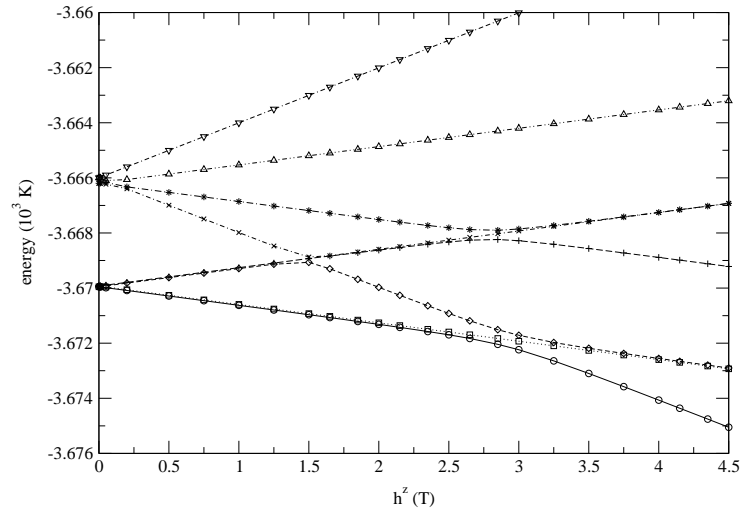


FIG. 9. Energies of the eight-state manifold vs. h^z , $D^x=100$ K, $D^y=D^z=0$ K.

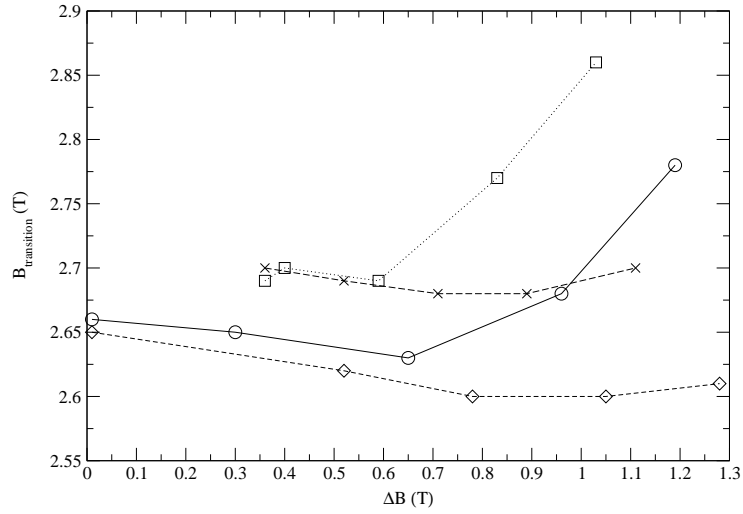


FIG. 10. Midpoint $B_{transition}$ versus width ΔB of the magnetization transition.
(I) $D^y=D^z=0$, left to right: $D^x = 0, 25, 50, 80, 100$ K, \circ : $T = 10^{-3}$ K, \square : $T = 0.1$ K
(II) $D^z=100$ K, left to right: $D^y=0, 20, 30, 40, 50$ K, \diamond : $T = 10^{-3}$ K, \times : $T = 0.1$ K.

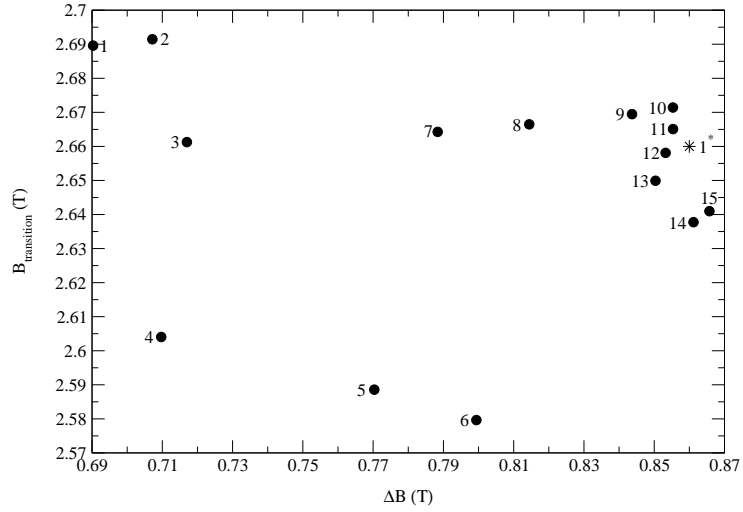


FIG. 11. Effect of $\Gamma_{i,j}$ on $B_{transition}$ and ΔB . Each point corresponds to a different $\Gamma_{i,j}$ according to table II. $\Gamma_{i,j} = \mathbf{0}$ for point 1*.

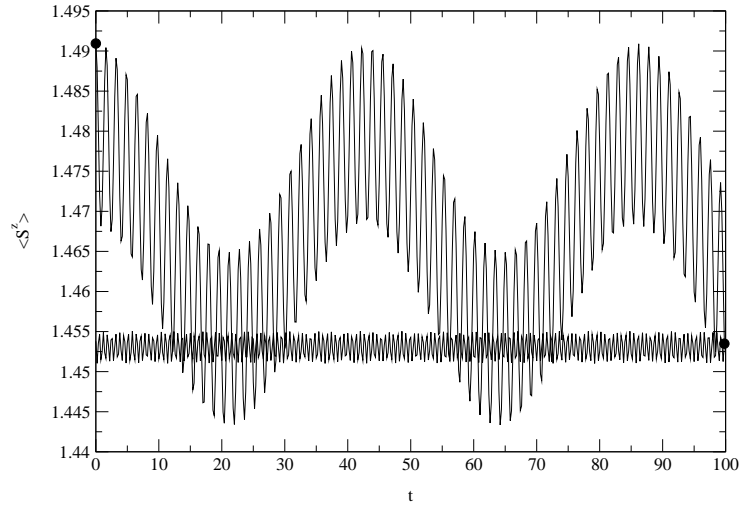


FIG. 12. $\langle S^z \rangle$ vs. time, time in units of $\tau_0 = \frac{\hbar}{k_B K} = 7.64 \times 10^{-12}$ s, $T = 0$, $D^x = 80$ K, $D^y = 30$ K, $D^z = 0$ K: “upper” solid line: after the field is switched off, “lower” solid line: field switched back on to 10 T. The black circles indicate $\langle S^z \rangle$ at the moments where the field is switched off and back on.